Basin and Range Province Seismic Hazards Summit III

Utah Geological Survey and Western States Seismic Policy Council

Invited Paper

Guide to Luminescence Dating Techniques and Their Application for Paleoseismic Research: *Harrison J. Gray, Shannon A. Mahan, Tammy Rittenour, and Michelle S. Nelson*

GUIDE TO LUMINESCENCE DATING TECHNIQUES AND THEIR APPLICATION FOR PALEOSEISMIC RESEARCH

Harrison J. Gray [1, 2*], Shannon A. Mahan [1], Tammy Rittenour [3, 4], and Michelle S. Nelson [3]
[1] U.S. Geological Survey, Luminescence Geochronology Laboratory, Denver, Colorado
[2] Cooperative Institute for Research in Environmental Sciences, University of Colorado, Boulder, Colorado
[3] USU Luminescence Laboratory, Utah State University, Logan, Utah
[4] Department of Geology, Utah State University, Logan, Utah
Senior author's email hgray@usgs.gov

ABSTRACT

Over the past 25 years, luminescence dating has become a key tool for dating sediments of interest in paleoseismic research. The data obtained from luminescence dating has been used to determine timing of fault displacement, calculate slip rates, and estimate earthquake recurrence intervals. The flexibility of luminescence is a key complement to other chronometers such as radiocarbon or cosmogenic nuclides. Careful sampling and correct selection of sample sites exert two of the strongest controls on obtaining an accurate luminescence age. Factors such as partial bleaching and post-depositional mixing should be avoided during sampling and special measures may be needed to help correct for associated problems. Like all geochronologic techniques, context is necessary for interpreting and calculating luminescence results and this can be achieved by supplying participating labs with associated trench logs, photos, and stratigraphic locations of sample sites.

INTRODUCTION

Luminescence dating is commonly applied to studies of late Quaternary deposits (Rhodes, 2011) as the minerals involved are ubiquitous on Earth's surface. In geologic settings, luminescence provides an estimate of the time elapsed since the last exposure of sand and silt grains to sunlight, which is assumed to have occurred during sediment transport. Thus, the luminescence age is effectively the depositional age of the sediment. The technique builds off the unique property of quartz and feldspar crystal lattices to "trap" and store free electrons that have been displaced by exposure to natural background radiation (Aiken, 1998). These trapped electrons remain locked in defects in the crystal lattice until an external source of energy such as heat, pressure, or light, provides the electrons the necessary energy to escape the lattice traps. The process of removal of previously held electrons, particularly by sunlight, is called bleaching.

Luminescence is complementary to other chronometers such as radiocarbon dating for two significant reasons. First, its application can be ideal for some settings because it does not require the presence of organic material for dating, leading to a wider range of potential sample material than available with radiocarbon dating (Bronk-Ramsey, 2014). Second, luminescence dating is typically able to date targets older than the maximum age range of radiocarbon (>40 ka), and in favorable environments, quartz optically stimulated luminescence (OSL) and feldspar infrared stimulated luminescence (IRSL) dating can extend back to 100-300 ka (Murray and Olley, 2002; Rittenour, 2008). The upper limit of luminescence dating stems from the finite number of traps available to store electrons; traps can become saturated and unable to record additional time. The time from deposition of the sediment to luminescence saturation depends on the level of defects in the crystal lattice and the background radiation dose rate, which, in turn, depends on the concentrations of potassium (K), uranium (U), and thorium (Th) in the surrounding sediments. In practice, luminescence dating uses dose-response measurements to calculate the number of stored electrons (the natural or equivalent dose), and divides this number by the trapping rate (the background radioactivity or dose rate) to produce the time since exposure to light or heat.

Given the applicable age range and ubiquity of quartz and feldspar in sediments, luminescence dating has become a vital tool for characterizing seismic hazards. For example, over the past 25 years, luminescence dating has been used in paleoseismic research to quantify surface-faulting earthquake timing, earthquake recurrence intervals (mean repeat time of earthquakes), and fault slip rates (e.g., Rhodes, 2011; McAuliffe and others, 2013; Fattahi, 2014). Moreover, the use of luminescence dating in paleoseismic studies has increased significantly in the last decade in response to new mandates to classify faults as active if they have experienced movement during the past 11 ka (e.g. California's Alquist-Priolo Earthquake Fault Zoning Act of 1972, revised most recently in 1993). Determining the timing of past surface-faulting earthquakes is especially important in cases where there are no historical observations of fault activity.

Luminescence methods and their application in paleoseismology have evolved over the past three decades. Early studies utilized thermoluminescence (TL) dating, which was the only method available prior to OSL and IRSL (Wintle and Huntley, 1982; Aiken, 1985) as a means to determine depositional age (Allen, 1986; Forman and others, 1990), and often in combination with radiocarbon ages (Jackson, 1991; McCalpin and Forman, 1991; a review in Fattahi, 2009). In particular, the Wasatch fault zone has been the site of many pioneering efforts (Forman and others, 1989, 1991; McCalpin and Forman, 1991; Stafford and Forman, 1993), which led to wider and global adoption of the methodology (Hall and others, 1994; Hansen and Lettis, 1994; Deng and others, 1996; Porat and others, 1996; Menges and others, 1997; Little and others, 1998; Galadini and Galli, 1999; Rockwell and others, 2000). The use of TL dating in paleoseismic research was largely replaced in the late 1990s by IRSL on polymineral silt (Porat and others, 1997; Personius and Mahan, 2000), and OSL on quartz sand (Zilberman and others, 2000; Lee and others, 2001) owing to the discovery of easier-to-bleach IRSL and OSL signals compared to TL (Huntley and others 1985; Aiken, 1998; Forman and others, 2000). In addition, the invention of the single aliquot regeneration (SAR) protocol (Murray and Wintle, 2000; Wallinga and others, 2000), and technological improvements allowing the measurement of single grains (Duller and others, 1999; Bøtter-Jensen and others, 2000) led to a rapid increase in the precision, accuracy, and applicability of luminescence techniques (Murray and Roberts, 1997; Duller, 2008; Rittenour, 2008). Consequently, the number and spatial distribution of paleoseismic studies using luminescence has risen significantly over the past 15 years (Korea: Cheong and others, 2003; Greece: Caputo and others, 2004; Vietnam: Zuchiewicz and others, 2004; Iran: Fattahi and others, 2006; Utah: Hylland and others, 2012; California: Briggs and others, 2013; McGill and others, 2013; Gold and others, 2014; Sohn and others, 2014).

At present, the standard for luminescence geochronology in paleoseismic research is quartz SAR OSL because quartz is easily bleached (~2 seconds, Godfrey-Smith and others, 1988), and because the SAR method provides a routine procedure for multiple luminescence measurements (Rhodes, 2011). TL and IRSL are still in use for cases where a sample is not conducive to quartz OSL, but are less favorable due to a harder-to-bleach signal (~1 minute or more), and the common phenomenon of anomalous fading in feldspars, which is the loss of luminescence signal over time. Innovations such as the development of thermal transfer OSL (TT-OSL; Wang and others, 2006) show promise to extend the age range of luminescence over an order of magnitude (Duller, 2012). Additionally, the development of the post-IR IRSL technique (pIRIR; Buylaert and others, 2009) allows for measurement of more stable feldspar signals that are useful in regions where quartz OSL have been found to be problematic due to geochemical reasons, such as in southern California (Lawson and others, 2012). Single grain options for both quartz OSL (Murray and Roberts, 1997) and for feldspar IRSL or pIRIR (Reimann and others, 2012) allow for statistical isolation of signals from only the best-bleached grains and more robust age determinations in otherwise hard-to-date deposits.

METHODS

Field Collection: Site Considerations

This section covers the fundamentals of luminescence sample collection in environments common in paleoseismology, such as trenches and incised alluvial fans. Sample collection for paleoseismic studies does not deviate significantly from the methods used in other applications of luminescence dating, but additional consideration is commonly needed prior to sampling in trench excavations (figure 1).

The selection of a target horizon for luminescence dating depends on the purpose and/or hypotheses of the study (Rhodes, 2011; Fattahi, 2014). Fortunately, luminescence is flexible because the method allows direct dating of a sedimentary body regardless of the presence of organic material (e.g. radiocarbon dating), assumptions of minimal erosion (cosmogenic surface exposure dating), or accumulation of post depositional minerals such as pedogenic carbonates. However, prior to sampling, a few principles must be considered.

First, the target unit must contain quartz and/or potassium feldspar in either the fine to very-fine sand range (250-63 µm grain size). Alternatively, the target unit can contain silt (~5-10 µm). This is generally an easy criterion to meet owing to the prevalence of these minerals and grain-size range in many geologic environments. In some regions, this may be a challenge due to the source geology. For example, alluvial fans adjacent to the Wasatch fault zone in Utah, contain dominantly carbonate rock with limited sources of siliciclastics. Similarly, many regions of southern California and Alaska contain abundant quartz that is geochemically unsuitable for luminescence dating (Jeong and Choi, 2011; Sawakuchi and others, 2011; Lawson and others,

Figure 1. *(A) Typical paleoseismic trench in a coarse alluvial-fan setting. (B) Example luminescence age sampling location on the trench wall. Note the sample is in a sandy layer between coarse, poorly sorted layers. Sample site hole is approximately 15 cm in diameter. Hole is larger than tube used for sampling.*

2012). In these cases, suitable material can be found as windblown dust inputs into the sedimentary deposits, or by the use of feldspar as an alternative to quartz. For coarse-grained alluvial fans such as those commonly studied in paleoseismology, it is generally favorable to target fine-grained layers within the fans rather than coarse deposits.

Second, the target sediment must have had sufficient exposure to sunlight before sediment burial such that any prior luminescence signal was depleted. The incomplete removal of a previous signal causes the apparent luminescence age to overestimate the depositional age (Jain and others, 2004). This process, called partial bleaching, is analogous to inheritance in the cosmogenic system (Anderson and others, 1996), or inherited age in radiocarbon (Frueh and Lancaster, 2014). Although this can be a limiting factor in determining an age, it can be mitigated by sampling strategies and analytical techniques. To minimize the possibility of sampling partially bleached sediment, one should target well-sorted sandy sediments with sedimentary structures indicative of low energy environments. Although common in alluvial-fan environments, poorly sorted debris flows are not ideal for luminescence dating because matrix sediment may not be exposed to sunlight during deposition. Colluvial wedges, which consist of sediment eroded from a fault scarp following surface faulting, can provide an optimal target for dating. However, to limit the sampling of only partially bleached sediment from the hanging wall (e.g., sediment transported only a limited distance), one should sample the toe of colluvial wedges and not deposits immediately abutting the fault plane (Porat and others, 2008). Modern analytical techniques, such as single-grain dating, which minimizes averaging of various luminescence signals when using small aliquots (Duller, 2008; Rittenour, 2008) can help identify partially bleached samples. Additionally, the use of mathematical treatments such as the minimum-age model (Galbraith and others, 1999; Galbraith and Roberts, 2012) allow for a robust statistical analysis of the most probable and most recent depositional age. Identification and evidence for partial bleaching is discussed in the data analysis section.

Third, the presence of bioturbation and pedoturbation should be avoided when possible; although, this may be infeasible in a fault trench where loose sediments are often attractive sites for animals and plants to penetrate into the deposit. Generally, turbation by plants and burrowing animals/insects serves to transport grains vertically throughout a sedimentary column (Bateman and others, 2003, 2007). Translocated grains will mix older or younger populations into the target unit introducing large uncertainties into the age determination. Common agents of turbation include plant roots, burrowing mammals, ants, and soil processes such as illuviation and/or eluviation. Statistical methods such as the finite mixture model (FMM; Galbraith and Green, 1990) can be used to identify mixed populations of grains, but do not commonly indicate the true burial age. Avoid potential mixing sites by targeting units with original and intact sedimentary structures (such as cross bedding) and without indicators of turbation (such as burrows, krotovina, or well-developed soil structure). In many cases, massive sediments have been turbated and therefore should be avoided, although due to grain-scale migration associated with roots, small insects, and pedogenic processes, mixed signals can also originate from deposits that appear intact. One case where it is preferable to target these units is when a buried soil is located between otherwise unfavorable units. The turbation that would have been occurring in the soil can generate a population of bleached grains which can be isolated for age determination.

Fourth, it is strongly preferable to select a sample that has had a consistent background radiation dose rate over the period of deposition (Aitken, 1998). Key to managing this is to locate sites that have not had large changes in the concentration of radioisotopes of K, U, and Th, or loss/addition of parent/daughter products, termed radioactive disequilibrium. Processes that can create disequilibrium include translocation of sediment via bio/pedo-turbation, loss of gaseous daughter products such as radon, and changes in the water content of the target sediment (Olley and others, 1996) by water table lowering or rising (often indicated by evidence of fluid flow such as secondary carbonate precipitation). As sediment is submerged below the groundwater table, U and K become mobile due to geochemical interactions, and can be removed by groundwater flow. Another form of disequilibrium is encountered with in-situ weathering of feldspar, which can mobilize K and alter the dose rate (Parish, 1994; Kawano and Tomita, 1996). Pedogenic processes that cause translocation and accumulation of clays (higher dose) and carbonates (lower dose) over time will also affect dose rates. These processes invalidate the assumption of constant dose rate with time and lead to large uncertainty in age estimates. Additionally, poorly sorted sediments, such as alluvial fans, can offer a large amount of heterogeneity in background radiation. To help place constraints on the background radiation dose rate, photos and sketches of the sample site are essential, and collection of cobbles representative of the surrounding lithology are useful in modeling point source variation in the dose rate. It is also extremely helpful to utilize a portable gamma spectrometer during field work, as the data collected at the site is often critical for determining changes in elemental concentrations in deposits with heterogeneous grain sizes (cobble to silt) common in paleoseismic trenches. Samples collected without portable gamma spectrometry data will incorporate significantly higher uncertainties into final age estimates.

Related to dose-rate considerations, one further issue is that the upper temporal limit on luminescence dating depends on the quantity of radioactive K, U, and Th (Wallinga, 2002) in the targeted deposit. Units with high concentrations of these values, such as boulder-rich alluvial fans sourced from granitic terrains, have younger temporal limits to dating than geologic units with carbonates, because carbonates are low in radioactive element concentrations. Conversely, sediments with low dose rates can produce heterogeneity in the radiation field due to differential dosing of grains near the dispersed radioisotopes within the sediment, causing greater scatter in the data (Mayya and others, 2006; Chauhan and Singhvi, 2011). However, it may be possible to circumvent these issues by modeling the dose rate through time (e.g., Lahaye and others, 2012).

Fifth, as faults can act as conduits for groundwater flow, this can result in fluctuations in the soil-moisture content of the sediment and influence the amount of radiation received by the sample. Water has two effects on the environmental dose rate: dilution and absorption (Aitken, 1985, 1998). In practice, this means that increased moisture content will reduce the environmental dose rate, resulting in an older luminescence age. Climatic variations in soil water content are especially dramatic in semiarid environments that experienced past pluvial periods (e.g. Nelson and Rittenour, 2014). Natural and man-made sediment exposures such as a fault trench are influenced by surface-drying effects, reducing soil moisture in the outer decimeter of the sediment-air interface. Over longer time scales, chemical weathering of clay minerals and mineral precipitation in pore spaces (i.e. carbonate) can alter the soil water content of a deposit through changes in porosity (Jeong and others, 2007; Nathan and Mauz, 2008). For these reasons, samples collected for measurement of in-situ moisture content can produce under- or over-estimates of the average sediment moisture content. It is important to ensure that original moisture conditions are being sampled, and to provide an estimation of average meteorological, climate, and groundwater conditions at the site (Crone and others, 2012).

One final consideration, is the exposure of the sample to cosmic radiation over the sample lifespan. Cosmic radiation is a component of the total dose rate (Aitken, 1998). It is preferable to sample units that have been at least one meter below the original geomorphic surface because cosmic radiation is exponentially attenuated with depth. At depths of less than one meter, small changes in burial depth from deposition or erosion will cause significant changes in the cosmic dose rate to the sample. If the target unit has experienced significant periods of time at different burial depths, as indicated by buried soils, then the relation to these depths should be documented along with other age control (Munyikwa, 2005; Lopez, 2012).

To summarize, luminescence dating targets must contain fine to very-fine (250-90 µm) quartz and/or feldspar-rich sand, or contain fine-grained silt (5-10 µm). Target units should have the greatest possible chance of grains receiving sunlight prior to deposition along their travel path no matter how short the path. Units with evidence of sediment mixing such as bioturbation should be avoided if possible. Sampling at depths greater than one meter is preferable in order to avoid errors from cosmic radiation. Finally, sites with a minimal (or a constant) amount of water content are preferred to avoid disequilibria in K, U, and Th concentrations.

Field Collection: Equipment and Methods

This section discusses sample collection methods commonly used in paleoseismic research. The guidelines presented here are focused toward sampling sandy, coarse-grained deposits such as alluvial fans, as these types of deposits frequently appear in tectonically active zones. The most common method of sample collection is by hammering a polyvinyl chloride (PVC) or steel tube into a sedimentary deposit. Alternative methods include manual collection of fine matrix material using canisters or collection by extracting a solid block from the outcrop. The necessary equipment used for sample collection for luminescence dating is outlined in table 1 and shown in figure 2.

Sampling may commence once conditions discussed in the prior section have been addressed, and the target sampling location has been determined. Note that copper, bronze, or aluminum tubes are often too weak to be driven into the sediment and buckle during sample collection. The size of the sampling tube should be appropriate for the size of the target unit, but large enough to ensure adequate sample is collected. The standard tube size mentioned in this paper is usually large enough to collect enough quartz for most lithologies. Smaller tubes increase the risk of not obtaining enough material to analyze. Collected samples should be sealed with duct tape and packed in a dark container or box and secured from sediment shaking during transport. Samples that are loose and not well packed within the tube can lead to mixing of the non-light exposed target grains with grains that were exposed to light at the ends of the tube. As a precaution, ship samples with a reputable carrier with tracking numbers and include a letter on official letterhead explaining the nature of the samples within the package.

Table 1. *Material and equipment used for luminescence sample collection via tube, canister, or block.*

Collection method:	Tube collection	Canister collection	Block collection
Target material:	• Non-cemented sand or silt beds • Interbedded sandy lenses in coarse-grained matrix	• Coarse-grained sediments absent of sandy lenses, but with silty or sandy matrix • Moderately cemented sediments	• Well-cemented or indurated sediments
Equivalent dose (D_E) sample container:	1. Sharpened opaque PVC or steel tubes with a plug inserted into the sharpened end to keep sediment compacted. 1.5-3” (3-8 cm) in diameter and 8” (20 cm) long, size may be dependent on target unit.	1. Light-tight container or bag for holding sample.	1. Large, plastic zip-locking bag or other material to cover and seal the block.
Field equipment for D_E and D_R collection:	2. A pounding cap or block of wood (wider diameter than the tube) and sledge hammer that can be used to pound against the cap or block.	2. Opaque blankets or tarps if collecting during daylight. Headlamp with red filter if collecting at night. Hand trowel or field shovel for removing exposed material and for filling canister.	2. Field knife or other hand tool for carving a block of indurated sediment out of the outcrop.
	3. Hand trowel for excavation, duct tape and/or rubber end caps for sealing ends of tube, and permanent marker for labeling.	3. Duct tape and tinfoil for sealing canister, and permanent marker for labeling.	3. Duct tape and tinfoil to secure and wrap the block and permanent marker for labeling. Black or silver spray paint (if desired). Do not use red or orange spray paint as it is not visible in the dark lab.
Dose rate (D_R) sample container:	4. Gallon-sized zip-locking bag to contain bulk sediment sample surrounding the tube.	4. Gallon-sized zip-locking bag to contain bulk sediment sample surrounding the DE sampling area.	4. N/A, this will be extracted from the outer (exposed) portion of the block.
Water content sample container:	5. Airtight container or zip-locking bags for water content sample.	5. Airtight container or zip-locking bags for water content sample.	5. N/A, this will be extracted from the outer (exposed) portion of the block.
Cosmogenic contribution:	6. Tape measure for depth below landform surface. GPS for latitude, longitude, and elevation.	6. Tape measure for depth below landform surface. GPS for latitude, longitude, and elevation.	6. Tape measure for depth below landform surface. GPS for latitude, longitude, and elevation.

Figure 2. *Possible sampling equipment. (1) Duct tape and aluminum foil. (2) Metal tubes and plastic/rubber end caps. (3) Field notebook. (4) Hammers, trowels, and wooden block to hammer against. (5) Measuring tape, permanent markers, photo scale, zip-locking bags. (6) Film canisters and light-proof bag. Light-proof bags can be obtained from a photography supply store.*

Tube Sampling Procedure

1. Prepare the tube by inserting a plug into the sharpened end of the tube (e.g., Styrofoam or aluminum foil) and sealing the unsharpened end with a cap and duct tape. This plug will prevent sediment mixing during pounding.

2. Position the sharpened end of the tube against the outcrop face; firmly hammer the tube into the outcrop while using a pounding cap or block of wood to absorb the impact (figure 3).

3. Cease hammering when the tube is flush with the outcrop face and the sample inside the tube is firmly and completely packed.

4. Uniformly excavate a representative sample of the sediment from ~30 cm around the sample tube, collecting it in a zip-locking bag (figure 3). Label and seal the bag with duct tape when around 600 grams of material is obtained. This sample will be used for dose-rate determination. If sediments are heterogeneous within 30 cm of the sample tube, then collect samples in separate bags and record the distance and geometry of the different beds sampled. Supply sketches and labeled photographs of the samples and dose-rate collection points. Alternatively, dose rate can be measured in the field with field-portable gamma spectrometer. A sample for water content determination should also be collected in an air-tight container.

5. Remove the sample tube from the outcrop and seal with a cap or aluminum foil and duct tape. If the sediment is not firmly packed into the tube, try either resampling with a clean tube or pack the end of the tube with something other than sand before sealing. Always label sample containers clearly and redundantly.

6. Record the latitude and longitude, elevation, the sample's depth below the ground surface (needed for cosmic dose rate contribution), submit photographs and trench logs of the sample location, and complete a lab sample submission worksheet (if applicable).

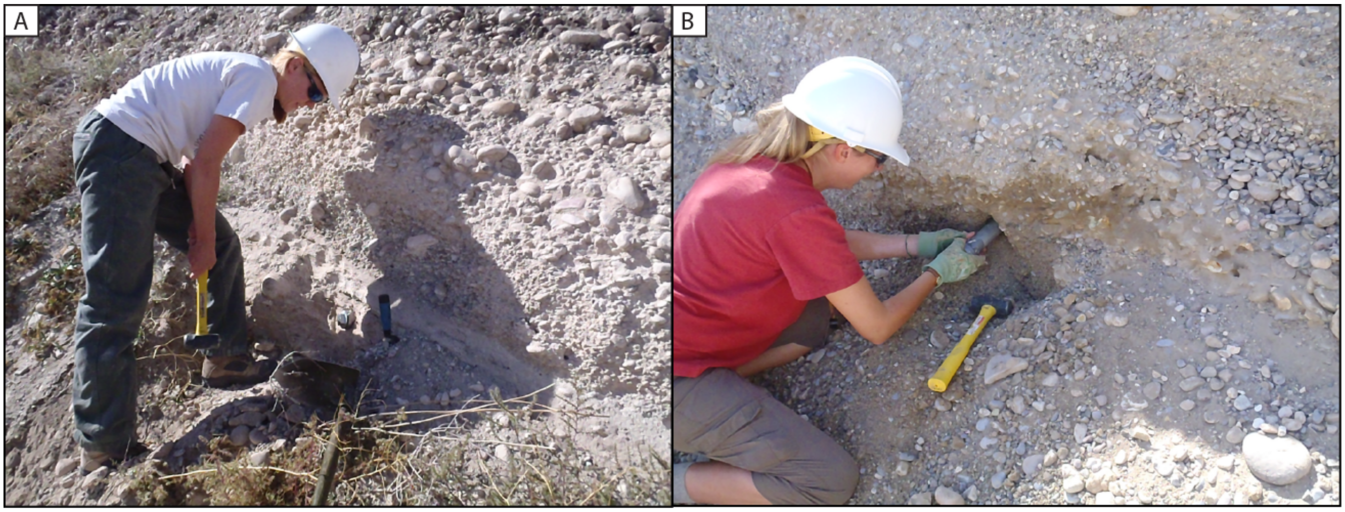

Figure 3. *(A) Example of tube collection of finer grained layer between moderately cemented coarse sediments. See text for detailed instruction. (B) After pounding into the outcrop, the tube is carefully extracted without allowing material to shift or fall out of the tube. The next steps are to collect a dose-rate sample, a sample for water content, measure the depth of the tube to the above surface, and to document the sample location (latitude, longitude, and elevation) and nearby sedimentology.*

Canister Collection

In some instances, it is impossible to sample using a tube, particularly in coarse or cemented sediments. As an alternative, a sample can be carefully collected and placed in a light-sealed container, such as a photo bag or film canister, if it is collected under dark conditions. This method of sampling is also useful if the target unit contains significant grain-size disparities such as cobbles and boulders with a silt matrix which preclude hammering in a tube, or if the tube is too large to sample a thin target layer. In contrast to the tube collection method, collection via canister requires a light-controlled environment to prevent bleaching during collection. Refer to table 1 for the list of equipment needed for sampling. As with tube samples, canister samples should be packed in a light-tight container or box, and secured from movement during transport.

Canister Sampling Procedure:

1. First, take photographs and make sketches of the sampling location, clearly describing the surrounding lithology.

2. Create a light-controlled environment by either covering the sampling site with opaque blankets or tarps to prevent possible bleaching during collection, or alternatively, sample during a moonless night to ensure a dark environment (figure 4).

3. Crawl under the blankets and confirm no light is entering the tent. Headlamps with special red-light filters available from outdoor supply stores may be used if shown to be luminescence-safe (figure 4).

4. Scrape away at least 5 cm of material on the outcrop surface to remove material that was previously exposed to light.

5. Carefully remove the unexposed sample from the outcrop and place in light-tight canister or bag. For coarse-grained units, target the fine-grained matrix material and avoid the edges of large clasts with weathering rinds. For thin units, a spoon or small trowel is useful to remove material.

6. Seal and label the canister or bag. If the sediment is not quartz or feldspar rich, collect more than one canister. The tarp can now be removed.

7. Collect material for the dose rate sample. Collect ~600 grams of representative material within a 30-cm radius of the sample location. For coarse-grained units, collect any large cobbles near the sample location and include with the bulk dose-rate sample. These can be broken in the field to reduce volume. Make sure to provide sketches and annotated photographs indicating sample location and location of dose-rate samples.

Figure 4. *(A) Example of canister collection. Here two individuals assist the sampling by draping an opaque tarp over the sample location as the finer grained matrix material is collected from around large clasts and immediately placed into a light-proof container. (B) In some instances, a dark blankets can be held in place on its own.*

Block Collection

Where the sediments are considerably indurated, or the other collection methods presented above are not practical, it is possible to collect a sample by block extraction. The block-extraction method involves the removal of a competent block of sediment from the outcrop, which is then taken back to the laboratory (table 1). Under dark lab conditions, the outer light-exposed layers are removed and the unexposed inner core is extracted for analysis. The recommended minimum size for a block is 15 x 15 x 15 cm. Larger-sized blocks improve the probability of successful extraction of enough sediment for dating once the outer several centimeters are removed for dose-rate and water-content samples. As with tube and canister sample collection, the block must be handled carefully and securely stored for transport. Any disintegration of the block, such as splitting in half before carefully wrapping, will compromise the sample for dating. It is best to carefully secure samples in hard-sided containers for transport. Spray painting the outer surface of the block with black or silver paint prior to wrapping it in bags and tape will help the lab to check the integrity of the sample.

Block Sampling Procedure:

1. Using a hand tool, outline as a minimum, a square of dimensions 15 x 15 cm for extraction of the block.

2. After outlining the block, proceed with removing material around the block continuing past the 15-cm maximum depth of the required block size.

3. Extract the block, spray paint around the outside faces, place the block in a bag or cover with aluminum foil, and duct tape the outside until secure. This does not need to be done as fast as possible as the outer light-exposed and spray-painted material will be removed in the lab.

4. Sketch, photograph, and record the site details including depth below the geomorphic surface.

Laboratory Preparation Overview

Laboratory preparation is aimed at exacting pure sand-sized grains of quartz or feldspar or polymineral fine silt for analysis. To achieve this, a series of mechanical and chemical separations are performed under red or amber safe-light conditions, each removing unwanted minerals and grain sizes. The general sequence of preparation is as follows, though some details vary depending on the laboratory. First, the sample is successively treated with hydrochloric acid to remove carbonates and with hydrogen peroxide to remove organic material. The sample is then sieved to separate the grain size of interest (usually in the 250–63 µm range), or to isolate silt if desired. Following sieving, the sample is dried and subject to a magnetic separation to remove iron-bearing minerals. This is typically performed with a Frantz magnetic separator. The sample is now largely composed of quartz and feldspar, which are separated by suspension in a high-density liquid (such as lithium heteropolytungstate) in which quartz sinks by gravity and feldspar remains in suspension. The feldspar extract is then ready for analysis. For quartz OSL dating, the quartz extract is subject to a treatment in concentrated hydrofluoric acid to remove any remaining feldspars and etch the outer 10% of the grains. The purified quartz or feldspar grains can then be loaded onto discs for single-aliquot or single-grain analysis. The previously isolated silt is mixed with methanol and pipetted as a slurry onto the discs. The discs are held at the bottom of a glass vial and subjected to heat to drive off the alcohol and leave the silt evenly plated on the discs. The silt is then ready for analysis.

Bulk samples collected from the sediment surrounding the sample are used to determine the background radiation dose rate. The dose rate can be measured in multiple ways: via high-purity germanium high-resolution gamma spectrometry (HPGe), by inductively coupled plasma mass spectrometry (ICP-MS), by instrumental neutron activation analysis (INAA), or by alpha- and beta-particle counting. Preparation of the material for each technique varies. Additionally, some laboratories have the capacity to measure elemental concentrations in the field with a portable sodium iodide (NaI) gamma spectrometer, or via emplacement of a capsule that contains an activated phosphor. Finally, determination of the moisture (water) content of the sample is performed by taking a small amount of material from the tube or a separate sample in an air-tight container and measuring the weight before and after drying. Modeling fluctuations in moisture conditions over the burial history may be necessary for samples that have undergone drainage (i.e. upthrown sediments) or saturation (i.e. downthrown sediments), or samples that are derived from alluvial deposits spanning the Pleistocene-Holocene boundary (Kenworthy and others, 2014). The values from these measurements are later used to calculate an age.

Data Analysis

After the sample has been treated and purified, the sediment is ready for analysis. Typically luminescence measurements are made on an automated device equipped with a radiation source, photomultiplier tube, and stimulating blue or infrared light-emitting diodes (LEDs). Analysis information is provided by the lab for inclusion in a publication. The sample is usually subject to the SAR protocol (Murray and Wintle, 2000), which involves measuring the natural luminescence signal followed by a series of irradiations and stimulation measurements to calibrate the individual luminescence response of an aliquot or single grain of sand to a given dose of radiation. These measurements are used to relate the natural luminescence signal to a dose of radiation, in units of Grays (Gy) where 1 Gy = 1 Joule/kg. This dose of radiation is called the *equivalent dose* (D_E). The D_E is then divided by the background radiation dose rate (D_R) to obtain an age following the equation:

The D_E is calculated from the measurement of tens to hundreds of aliquots or hundreds to thousands of single grains. These measurements compose the majority of time required for age analysis, and are the reason why luminescence dating is so time consuming. In general, it takes about one week of dedicated instrument time per sample to calculate a representative D_E for the calculation of a luminescence age. Due to large backlogs at most labs, turnaround times are typically well over six months.

Unlike radiocarbon dating where only one measurement is made on each sample, many measurements of D_E are required for luminescence dating because there is often significant variation in D_E between aliquots and grains. Statistical models are applied to determine the appropriate D_E for age determination. There are several age models available for D_E calculations. Commonly used age models include the central age model (weighted mean), minimum age model (selects the youngest population of grains), and the finite mixing model (identifies discrete populations of grains). The choice of model depends on the D_E distributions with the primary caveat that the D_E value most commonly sought is that of the grains exposed to sunlight most recently within the deposit of interest (figure 5A, 5B, and 5C; Galbraith and Roberts, 2012). It is important to note that statistical modeling should not be conducted in isolation from the depositional context of a sample, stratigraphic considerations, or other germane information, such as independent age control.

Once the D_E data have been measured, luminescence practitioners quantify the results for three reasons: (1) to understand the population characteristics of the sample (size, mean, standard deviation), (2) to define the distribution parameters of disper-

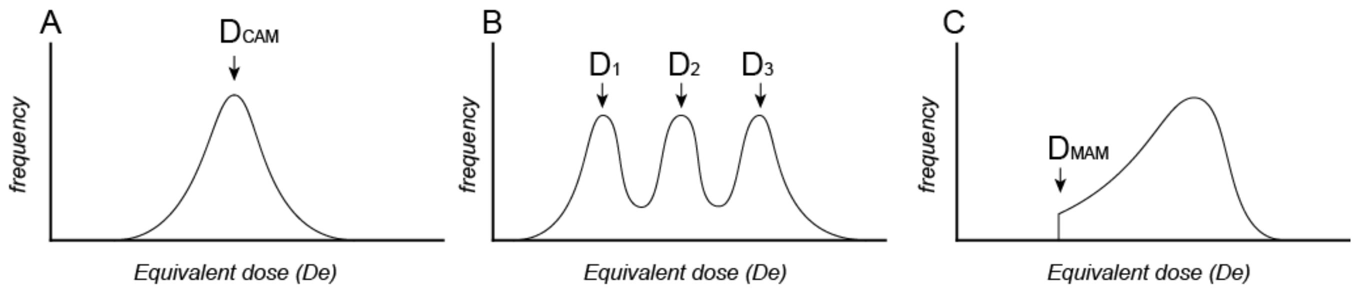

Figure 5. *Schematic equivalent dose distributions and the use of the appropriate age model for each condition. (A) Example of an originally well-bleached sample with a single age population. The label and arrow (DCAM) demonstrate the application of the Central Age Model (CAM), which computes a weighted mean at the peak of the normal distribution. (B) Example of a sample with various age populations possibly introduced by various bleaching histories or post-depositional mixing. This situation is appropriate for the Finite Mixing Model (FMM) which can statistically identify each age population (D1, D2, D3). (C) Schematic example of a partially bleached sample where insufficient sunlight exposure removed the signal of only a few select grains. Label and arrow (DMAM) indicate population isolated by the Minimum Age Model (MAM). Adapted from Duller (2008).*

sion (or overdispersion), skewness, and kurtosis, and (3) to identify the sources of random and systematic error. This understanding of the D_E distribution is often used to decide which age model to use to calculate the age of a sample. A summary of the statistical aspects of D_E and error calculation in OSL dating can be found in Galbraith and Roberts (2012).

Many labs commonly report the dispersion or overdispersion in a data set with final results. Dispersion is scatter or variation due to Poisson variation; that is, the scatter beyond that due to the estimation error associated with each observed measurement. However, the term overdispersion is used more generally to describe observations that vary more than they should, according to an assumed statistical model. Galbraith and Roberts (2012) suggest that an overdispersion parameter of about 23% is typical of many types of sediment measured for luminescence. Labs will also commonly report the skewness of the D_E data if the samples display evidence for partial bleaching, which is expected to produce positively skewed D_E distributions with the youngest population reflecting the grains that were fully bleached at deposition (Bailey and Arnold, 2006).

Uncertainties in luminescence age calculations are typically based on the standard error of the D_E data set, as well as propagated random and systematic error from dose-rate calculation and instrumental calibration. Errors are summed in quadrature (square root of the sum of the square of the errors) and are reported at the one-sigma level (68% confidence level). All luminescence ages should be reported with errors that incorporate both random and systematic errors so they are comparable between labs and techniques (Lepper and others, 2011).

The accuracy of luminescence ages depends on a number of parameters. As discussed above, it is essential that as much measurement information as possible is included in any report or publication dealing with luminescence ages because of the various limitations on the precision of luminescence ages. When uncertainties in the measurement of the D_R, often dominated by issues of water content, and D_E are combined, errors quoted on luminescence ages typically range from 5 to 10%, including both random and systematic sources of error. However, precision of individual samples can be much lower due to partial bleaching and luminescence signal strength.

Some sources of error common to all luminescence samples (systematic errors) include conversion from concentration data to D_R (estimated at ~3%), absolute calibration of concentration measurements (~3%), beta source calibration (~2%), and beta attenuation factors (~2%). These estimated values are of course approximate, but it should be clear that it is difficult to obtain a luminescence age with an overall or combined standard uncertainty of much less than 5% (Duller, 2007a). This is especially true when noting that other sources of systematic error have not been commonly considered because they are site dependent, and that uncertainties arising from random errors also contribute to the combined standard uncertainty (Duller, 2007b; Galbraith and Roberts, 2012).

Laboratory results are often presented as a table including the estimated water content, concentrations of radionuclides, cosmic and background D_R, D_E, and finally, the luminescence age (table 2). The information provided by the analyzing lab should also contain any additional information used to determine the luminescence age, such as the dating method used, mineral and grain size analyzed, preheat-plateau and dose-recovery test results, the age model used, and assumptions about water content through time.

Table 2. *Example of a common data table produced by a luminescence study.*

Sample information	% Water content[a]	K (%)[b]	U (ppm)[b]	Th (ppm)[b]	Cosmic dose (Gy/ka)[c]	Total Dose Rate (Gy/ka)	Equivalent Dose (Gy)	n[d]	Scatter[e]	Age (ka)[f]
Sample 1	1 (32)	3.89 ± 0.05	3.50 ± 0.18	28.8 ± 0.39	0.24 ± 0.02	7.16 ± 0.08	423 ± 70	11 (16)	45.0	59.1 ± 9.8
Sample 2	7 (38)	4.07 ± 0.04	4.23 ± 0.14	30.9 ± 0.41	0.23 ± 0.02	7.16 ± 0.07	657 ± 34.2	15 (17)	41.1	66.2 ± 6.7

[a] Field moisture, with figures in parentheses indicating the complete sample saturation %. Ages calculated using field moisture values.

[b] Analyses obtained using laboratory gamma spectrometry (low resolution NaI detector for the 2007 samples and high resolution Ge detector for the 2012 samples).

[c] Cosmic doses and attenuation with depth were calculated using the methods of Prescott and Hutton (1994). See text for details.

[d] Number of replicated equivalent dose (De) estimates used to calculate the mean. Figures in parentheses indicate total number of measurements made including failed runs with unusable data.

[e] Defined as "over-dispersion" of the De values in %. Obtained by taking the average over the std deviation. Values >35% are considered to be poorly bleached sediments.

[f] Dose rate and age for fine-grained 250-180 microns quartz. Exponential fit used on equivalent dose, errors to one sigma, ages and errors rounded. Equivalent dose populations used for ages based off Minimum age model (Galbraith and others, 1999).

Previously, results were commonly presented graphically via histograms and/or probability density plots (figure 6A, figure 6B; Duller, 2008). Histograms group or bin data into sets that have similar values and display them as columns with heights proportional to the number of contained values. Histograms have fallen out of usage due to their inability to express the precision of individual equivalent dose estimates, and the misleading visual effects created by bin widths that are arbitrarily chosen (Duller, 2008; Galbraith and Roberts, 2012). Probability density plots (Hurford and others, 1984; Lowell, 1995; Brandon, 1996) allow for the display of individual uncertainties and the relative probabilities of individual ages similar to kernel density estimates. The "probability density plot" incorporates D_E values and associated uncertainty as individual Gaussian distributions, which are then summed to produce a single curve of total probability. Estimates of D_E with high precision are displayed as narrow and tall Gaussian curves, while low-precision estimates produce shorter and broader curves. The probability density plot can; however, be misleading as the total curve places greater weight on precision than on accuracy, and the peaks of the curve may not reflect true age components (Galbraith, 1998).

Today, luminescence studies typically use radial plots to display D_E values (Galbraith, 1988, 1990). Radial plots display both individual D_E values (plotted on the radial axis) and their associated precision (plotted on the x-axis) (figure 6C). Radial plots display data as a scatter plot, where data points that are of similar age or equivalent dose are plotted along a radial line emanating from the origin on the left-hand side of the plot. Additionally, two-sigma error bars can be placed on the radial plot to illustrate data points within error of a selected value, typically the value of the selected age model. Dispersion in the data is shown by data points that lie outside the two-sigma region. Radial plots are common in the luminescence literature, but have a slight disadvantage when plotting zero age samples as the logarithm of the age is needed to construct the plot (Duller, 2008).

DISCUSSION

The successful application of luminescence dating first and foremost depends on collecting suitable samples. Paleoseismologists working in trenches are at a disadvantage compared to other applications of luminescence dating because they have to sample what is revealed in the trench, and have no choice about the sediments other than those sediments that were deposited in relationship to the fault. Sampling within trenches is often further limited by access and time constraints, as many trenches are filled in after study. Therefore, it is preferred that a luminescence specialist visit the trench to sample, or if that cannot be arranged, is provided access to trench logs, stratigraphic context documentation (such as field notebooks or digital maps), and photos of the sediments sampled. There are many studies that show that with proper selection of sediments from a paleoseismic context, luminescence dating can provide reliable ages (Fattahi, 2014) even in the most difficult field settings.

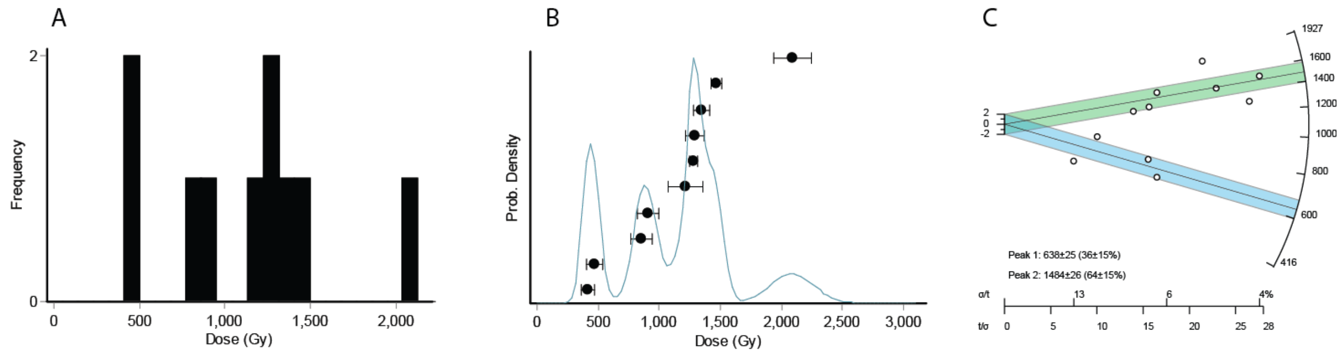

Figure 6. *Examples of graphical presentation of luminescence data. (A) histogram and (B) weighted histogram produced by Luminescence Analyst v. 4.1 (Duller, 2007); C) radial plot generated using Radialplotter v. 7.1 (Vermeesch, 2009). See text for discussion of advantages and disadvantages associated with each plot type.*

For almost all paleoseismic investigations, quartz OSL is the preferred method as it is most likely to be bleached at the time of deposition given short transport distances. Typical saturation age ranges for quartz are 50-200 ka (Murray and Olley, 2002; Rhodes, 2011; Mahan and others, 2014). However, there may be cases where the unit in question is very old or the D_Rs are considerably high, in which case it may be preferable to use a technique such as TT-OSL on quartz or pIR-IRSL on feldspar. These methods have higher maximum age limits (>200 ka), but frequently contain large residual doses at deposition. In some cases, the burial age is old enough that these residuals are insignificant, or can be subtracted via measurements of residual doses. The upper age limit also depends on the background D_R. Higher D_Rs serves to fill electron traps faster than lower D_Rs. Generally, more mature sedimentary units (i.e. those having increased sorting and dominance of quartz over other minerals), such as eolian or beach sands, have lower D_Rs than less mature units such as alluvial-fan deposits.

Partial bleaching, the incomplete removal of a prior signal due to insufficient sunlight-exposure, is one of the most commonly encountered problems in luminescence dating (Aitken, 1998; Jain and others, 2004). Partial bleaching serves to make grains appear older than the most recent depositional episode. The presence of a few unbleached grains can be significant enough to increase the apparent age of an entire aliquot or sample (Olley and others, 1999). The variety of rates and mechanisms of grain transport can lead to vast differences in the amount of sunlight exposure experienced by each grain. Floods, debris flows, and other processes that involve rapid transport in turbid conditions are prone to limited signal resetting. Additionally, the attenuation of light through water can drastically change the rates of bleaching (Kars and others, 2014). Fortunately, methods such as single-grain analysis and statistical models such as MAM provide a means to isolate the best bleached grains (Rittenour, 2008). The use of OxCal (Lienkaemper and Bronk-Ramsey, 2009; Bronk-Ramsey, 2014) or other Bayesian programs that provide outlier analyses and chronological ordering linking multiple samples or sites is outside the purview of this paper, but such statistical modeling is commonly used in paleoseismic research, and can include luminescence results (e.g., Lienkaemper and Bronk-Ramsey, 2009; DuRoss and others, 2011, Bronk-Ramsey, 2014). Because paleoseismic research occurs in a variety of environments, the potential bleaching of any given geologic unit can vary considerably. Trench sites near the base of mountain fronts (e.g. Crone and others, 2012) can be difficult, but not insurmountable in terms of identifying burial ages. A general rule of thumb is that the farther traveled and more sedimentologically mature a material (i.e., increased sorting, and dominance of quartz over other minerals), the more likely it is to be completely bleached (Jain and others, 2004).

One final consideration is the effect of bioturbation on target units. Bateman and others (2003, 2007) have demonstrated the effects that bioturbation and pedoturbation can have on luminescence signal distributions in sediment. As grains are moved vertically through a sediment column, the dispersion in luminescence values is expected to increase as foreign grains are incorporated into measurements. The distribution of D_E will show an increase in kurtosis and a possible change in the skewness depending on the mixing mechanism. The effect can be large when the mixing occurs for a long time period or when layers with drastically different signals are mixed (Bateman and others, 2003). One other consideration is that mixing can change the DR through time, but this may not be significant in most cases (Bateman and others, 2003). The identification of this mixing depends on both field observations and distributions of D_Es. Generally, mixed units should be avoided if the mixing has occurred long after the deposition of the unit. In cases of buried soils, the prior mixing can help bleach grains and can be useful for dating if mixing ceased after burial.

Evidence for changes in dosimetry over time and space due to changes in water content, additions or loss of radiogenic isotopes from pedogenic processes or turbation should be documented and described as accurately as possible before the trench is closed. Significant effort is expended on developing a robust model of the D_E, but calculation of the D_R is just as important and sometimes just as challenging as calculating the D_E. The use of a portable gamma spectrometer during the OSL sampling process in fault trenches greatly aids in the selection of the most probable elemental concentration to be paired with OSL, and can help avoid locations with disequilibria or extreme compositional heterogeneity (e.g., one of the readings is very different than the others; De Corte and others, 2004; Gu Cor and Mercier, 2011). Portable gamma spectrometry also helps overcome the effects of heterogeneous stratigraphy that are so common in fault trenches; after all, the reason for the paleoseismic study is because of stratigraphic anomalies. Several gamma spectrometer models are available for use, and it is helpful to partner with a luminescence expert that already has one or can evaluate the need for one.

Sediment with water contents near saturation will have much lower D_Rs than those that are dry. An increase of 5% in moisture contents increases the age by roughly 4% (Porat and others, 2012); therefore, accurate moisture estimates (Aitken, 1998) are important. Changes in average water content through time can lend a large, and ultimately unknown, amount of uncertainty to age estimates. However, this effect can be minimized with careful consideration of the site's paleohydrology, measurement of the sediment saturation, and field moisture using guidelines in Mahan and others (2014) and Nelson and Rittenour (2014). It is critical to collect samples for water content shortly after trenching a site, and to provide an estimate of average meteorological, climate, and groundwater conditions at the site. Because paleoseismic investigations occur in a variety of geomorphic settings, there is no specific set of guidelines, and each site and each trench should be analyzed on a case-by-case basis.

CONCLUDING REMARKS

Luminescence dating has been successfully applied to paleoseismic studies for the past 25 years and is progressing toward increasingly robust age determinations. Luminescence dating can be applied to virtually any fine-grained sediment containing quartz and feldspar sand or silt. A main strength of the technique for paleoseismology is that it allows great versatility in selecting sampling horizons, especially in depositional settings that lack significant organic deposits. When available, utilizing both radiocarbon and luminescence dating can produce robust results and provide a crosscheck for each method (Rittenour and others, 2014). Careful sampling and correct selection of sample sites exert two of the strongest controls on obtaining a robust and accurate luminescence age. Sampling procedures such as tube, canister, and block collection provide multiple options for sample collection from a wide range of sediments. When submitting samples, include as much information as possible, such as trench logs, stratigraphic context, and photos as significant amounts of information are present in a luminescence equivalent dose dataset. Like all geochronologic techniques, context is necessary for interpreting and calculating these luminescence results, and to assess the likely depositional age. A general rule of thumb is that the more sedimentologically mature a material is (i.e. greater sorting and quartz dominance), the greater the potential for complete bleaching. Environments which have been altered post-deposition, such as by bio/pedo-turbation or weathering via groundwater interactions, can complicate age determinations and should be avoided. One exception is when a soil is buried and the turbation prior to burial introduces bleached grains. Careful field collection and documentation is one of the most important factors in producing robust and meaningful luminescence ages.

ACKNOWLEDGMENTS

This manuscript benefited significantly from reviews provided by Rich Briggs and Chris DuRoss of the U.S. Geological Survey (USGS). Thank you both for polishing the discussion and methods and for refining the science behind the words. We would also like to thank the USGS TRIGA reactor team of Tim DeBey, Alex Buerhle, Brycen Roy, and Chris Farwell for providing countless gamma spectrometry measurements and for continued discusssion on the merits and configurations of gamma spectrometry dosimetry. We could not perform the science we do without the TRIGA Reactor Team. Any use of trade, product, or firm names is for descriptive purposes only and does not imply endorsement by the U.S. Government.

REFERENCES

Adamiec, G., and Aitken, M.J., 1998, Dose-rate conversion factors–update: Ancient TL, v. 16, no. 2, p. 37-50.

Aitken, M.J., 1985, Thermoluminescence dating: Oxford, Academic Press, 359 p.

Aitken, M.J., 1998, An introduction to optical dating—The dating of Quaternary sediments by the use of photon-stimulated luminescence: Oxford University Press, 267 p.

Allen, C.R., 1986, Seismological and paleoseismological techniques of research in active tectonics, *in* Active tectonics: Washington, DC: The National Academies Press, National Research Council Studies in Geophysics, p. 148-154.

Anderson, R.S., Repka, J.L., and Dick, G.S., 1996, Explicit treatment of inheritance in dating depositional surfaces using in situ ^{10}Be and ^{26}Al: Geology, v. 24, no.1, p. 47-51.

Bailey, R.M., and Arnold, L.J., 2006, Statistical modeling of single grain quartz D_e distributions and an assessment of procedures for estimating burial dose: Quaternary Science Reviews, v. 25, p. 2475-2502.

Bateman, M.D., Frederick, C.D., Jaiswal, M.K., and Singhvi, A.K., 2003, Investigations into the potential effects of pedoturbation on luminescence dating: Quaternary Science Reviews, v. 22, no. 10, p. 1169-1176.

Bateman, M.D., Boulter, C.H., Carr, A.S., Frederick, C.D., Peter, D., and Wilder, M., 2007, Detecting post-depositional sediment disturbance in sandy deposits using optical luminescence: Quaternary Geochronology, v. 2, no. 1, p. 57-64.

Berger, G.W., Rockwell, T.K., and Huntley, D.J., 1998, Paleoseismology from luminescence dating—Tests and application in Southern California, USA: Chinese Science Bulletin, v. 43, p. 8-8

Brandon, M.T., 1996, Probability density plot for fission-track grain-age samples: Radiation Measurements, v. 26, no. 5, p. 663-676.

Briggs, R.W., Wesnousky, S.G., Brune, J.N., Purvance, M.D., and Mahan, S.A., 2013, Low footwall accelerations and variable surface rupture behavior on the Fort Sage Mountains fault, northeast California: Bulletin of the Seismological Society of America, v. 103, no. 1, p. 157-168.

Bronk-Ramsey, C., 2014, Radiocarbon dating in paleoseismology, *in* Beer, M., Kougioumtzoglou, I.A., Patelli, E., Siu-Kui Au, I., editors, Encyclopedia of earthquake engineering: Springer Berlin Heidelberg, p. 1-11.

Bøtter-Jensen, L., Bulur, E., Duller, G.A.T., and Murray, A.S., 2000, Advances in luminescence instrument systems: Radiation Measurements, v. 32, no. 5, p. 523-528.

Buylaert, J.P., Murray, A.S., Thomsen, K.J., and Jain, M., 2009, Testing the potential of an elevated temperature IRSL signal from K-feldspar: Radiation Measurements, v. 44, no. 5, p. 560-565.

Chauhan, N., and Singhvi, A.K., 2011, Distribution in SAR palaeodoses due to spatial heterogeniety of natural beta dose: Geochronometria, v. 38, no. 3, p. 190-198.

Caputo, R., Helly, B., Pavlides, S., and Papadopoulos, G., 2004, Palaeoseismological investigation of the Tyrnavos fault (Thessaly, central Greece): Tectonophysics, v. 394, no. 1, p. 1-20.

Chen, R., and Pagonis, V., 2010, Thermally and optically stimulated luminescence—A simulation approach: West Sussex, John Wiley & Sons, United Kingdom, 434 p.

Cheong, C.S., Hong, D.G., Lee, K.S., Kim, J.W., Choi, J.H., Murray, A.S., and Chang, H.W., 2003, Determination of slip rate by optical dating of fluvial deposits from the Wangsan fault, SE Korea: Quaternary Science Reviews, v. 22, no. 10, p. 1207-1211.

Crone, A.K., Personius, S.F., DuRoss, C.B., Machette, M.N., and Mahan, S.A., 2012, Paleoseismology of the Willow Creek site and chronology of late Holocene earthquakes on the Nephi segment, Wasatch fault zone, Utah, *in* Hylland, M.D. and Harty, K.M, editors, Selected topics in engineering and environmental geology in Utah: Utah Geological Association Publication 41, p. 193-206, (CD).

De Corte, F., Umans, H., Vandenberghe, D., DeWispelaere, A., and Van den Haute, P., 2004, Direct gamma-spectrometric measurement of the 226Ra 186.2 keV line for detecting 238U/226Ra disequilibrium in determining the environmental dose rate for the luminescence dating of sediments: Applied Radiation and Isotopes, v. 63, no. 5-6, p. 589-598.

Deng, Q., Zhang, P., Xu, X., Yang, X., Peng, S., and Feng, X., 1996, Paleoseismology of the northern piedmont of Tianshan Mountains, northwestern China: Journal of Geophysical Research—Solid Earth, v. 101 no. B3, 5895-5920.

Duller, G.A.T., 2007a, Assessing the error on equivalent dose estimates derived from single aliquot regenerative dose measurements: Ancient TL, v. 25, p. 15-24.

Duller, G.A.T., 2007b, Analyst Manual, p. 1- 45.

Duller, G. A.T., 2008, Single-grain optical dating of Quaternary sediments—Why aliquot size matters in luminescence dating: Boreas, v. 37, no. 4, p. 589-612.

Duller, G.A.T., and Wintle, A.G., 2012, A review of the thermally transferred optically stimulated luminescence signal from quartz for dating sediments: Quaternary Geochronology, v. 7, p. 6-20.

Duller, G.A.T., Bøtter-Jensen, L., Kohsiek, P., and Murray, A.S., 1999, A high-sensitivity optically stimulated luminescence scanning system for measurement of single sand-sized grains: Radiation Protection Dosimetry, v. 84, p. 325-330.

DuRoss, C.B., Personius, S.F., Crone, A.J., Olig, S.S., and Lund, W.R., 2011, Integration of paleoseismic data from multiple sites to develop an objective earthquake chronology–Application to the Weber segment of the Wasatch fault zone: Bulletin of the Seismological Society of America, v. 101, p. 2765–2781.

Fattahi, M., Walker, R., Hollingsworth, J., Bahroudi, A., Nazari, H., Talebian, M., Armitage, S., and Stokes, S., 2006, Holocene slip-rate on the Sabzevar thrust fault, NE Iran, determined using optically stimulated luminescence (OSL): Earth and Planetary Science Letters, v. 245, no. 3, p. 673-684.

Fattahi, M., 2009, Dating past earthquakes and related sediments by thermoluminescence methods—A review: Quaternary International, v. 199, no. 1-2, p. 104-146.

Fattahi, M., 2014, Luminescence, earthquake, and tectonic activity, *in* Rink, J.W., and Thomas, J., editors, Encyclopedia of scientific dating methods: Springer, p. 1-8.

Forman, S.L., Machette, M.N., Jackson, M.E., and Maat, P., 1989, An evaluation of thermoluminescence dating of paleoearthquakes on the American Fork segment, Wasatch fault zone, Utah: Journal of Geophysical Research—Solid Earth, v. 94, no. B2, p. 1622-1630.

Forman, S.L., Pierson, J., and Lepper, K., 2000, Luminescence geochronology, *in* Sowers, J.M., Noller, J.S., and Lettis, W.R., editors, Quaternary geochronology, methods and applications: American Geophysical Union, Reference Shelf 4, p. 157-176.

Forman, S., Nelson, A.R., and McCalpin, J.P., 1991, Thermoluminescence dating of fault-scarp-derived colluvium—Deciphering the timing of paleoearthquakes on the Weber segment of the Wasatch fault zone, north central Utah: Journal of Geophysical Research, v. 96, no. 81, p. 595-605.

Frueh, W.T., and Lancaster, S.T., 2014, Correction of deposit ages for inherited ages of charcoal: implications for sediment dynamics inferred from random sampling of deposits on headwater valley floors: Quaternary Science Reviews, v. 88, p. 110-124.

Galadini, F., and Galli, P., 1999, The Holocene paleoearthquakes on the 1915 Avezzano earthquake faults (central Italy)—Implications for active tectonics in the central Apennines: Tectonophysics, v. 308, no. 1, p. 143-170.

Galbraith, R.F., 1988, Graphical display of estimates having differing standard errors: Technometrics, v. 30, p. 271-281.

Galbraith, R.F., 1990, The radial plot—Graphical assessment of spread in ages: Nuclear Tracks and Radiation Measurements, v. 17, p. 207-214.

Galbraith, R.F., 1998, The trouble with “probability density” plots of fission track ages: Radiation Measurements, v. 29, no. 2, p. 125-131.

Galbraith, R.F., 2005, Statistics for fission track analysis: Boca Raton, Chapman & Hall/CRC Press, 240 p.

Galbraith, R.F., Roberts, R.G., Laslett, G.M., Yoshida, H., and Olley, J.M., 1999, Optical dating of single and multiple grains of quartz from Jinmium rock shelter, northern Australia—Part I, experimental design and statistical models: Archaeometry, v. 41, no. 2, p. 339-364.

Galbraith, R.F., and Green, P.F., 1990, Estimating the component ages in a finite mixture: International Journal of Radiation Applications and Instrumentation, Part D, Nuclear Tracks and Radiation Measurements, v. 17, no. 3, p. 197-206.

Galbraith, R.F., and Roberts, R.G., 2012, Statistical aspects of equivalent dose and error calculations and display in OSL dating—An overview and some recommendations: Quaternary Geochronology, v. 11, p. 1-27.

Godfrey-Smith, D.I., Huntley D.J., and Chen, W.H., 1988, Optical dating studies of quartz and feldspar sediment extracts: Quaternary Science Reviews, v. 7, p. 373–380.

Gold, R.D., Briggs, R.W., Personius, S.F., Crone, A.J., Mahan, S.A., and Angster, S. J., 2014, Latest Quaternary paleoseismology and evidence of distributed dextral shear along the Mohawk Valley fault zone, northern Walker Lane, California: Journal of Geophysical Research—Solid Earth, v. 119, no. 6, p. 5014-5032.

Guérin, G., and Mercier, N., 2011, Determining gamma dose rates by field gamma spectroscopy in sedimentary media—Results of Monte Carlo simulations: Radiation Measurements, v. 46, no. 2, p. 190-195.

Hall, N.T., Hunt, T.D., and Vaughan, P.R., 1994, Holocene behavior of the San Simeon fault zone, south-central coastal California, *in* Alterman, I. B., McMullen, R. B., Cluff, L. S., and Slemmons, D. B, editors, Seismotectonics of the central California Coast Ranges: Geological Society of America Special Paper 292, p. 167-190.

Hanson, K.L., and Lettis, W.R., 1994, Estimated Pleistocene slip rate for the San Simeon fault zone, south-central coastal California, *in* Alterman, I. B., McMullen, R. B., Cluff, L. S., and Slemmons, D. B, editors, Seismotectonics of the central California Coast Ranges: Geological Society of America Special Paper 292, p. 133-150.

Hurford, A.J., Fitch, F.J., and Clarke, A., 1984, Resolution of the age structure of the detrital zircon populations of two Lower Cretaceous sandstones from the Weald of England by fission track dating: Geological Magazine, v. 121, no. 4, p. 269-277.

Hylland, M.D., DuRoss, C.B., McDonald, G.N., Olig, S.S., Mahan, S.A., and Oviatt, C.G., 2012, Basin-floor Lake Bonneville stratigraphic section as revealed in paleoseismic trenches on the West Valley fault zone, Salt Lake Valley, Utah, *in* Hylland, M., and Harty, K., editors, Engineering and environmental geology of Utah: Utah Geological Association Publication 41, p. 175-193, CD.

Jackson, M., 1991, The number and timing of Holocene paleoseismic events on the Nephi and Levan segments, Wasatch fault zone, Utah—Paleoseismology of Utah, Volume 3: Utah Geological Survey Special Study 78, 23 p., 3 plates.

Jain, M., Murray, A.S., and, Botter-Jensen, L., 2004, Optically stimulated luminescence dating: how significant is incomplete light exposure in fluvial environments?: Quaternaire, v. 15, no. 1, p. 143-157.

Jeong, G.Y., Cheong, C., and Choi, J.H., 2007, The effect of weathering on optically stimulated luminescence dating: Quaternary Geochronology v. 2, no. 1, p. 117-122.

Jeong, G.Y., and Choi, J.H., 2011, Optically stimulated luminescence characteristics of granitoid quartz: Journal of the Mineralogical Society of Korea, v. 24, no. 4, p. 321-325.

Kars, R.H., Reimann, T., Ankjærgaard, C., and Wallinga, J., 2014, Bleaching of the post-IR IRSL signal—New insights for feldspar luminescence dating: Boreas, v. 43, no. 4, p. 780-791

Kawano, M., and Tomita, K., 1996, Amorphous aluminum hydroxide formed at the earliest weathering stages of K-feldspar: Clays and Clay Minerals, v. 44, no. 5, p. 672-676.

Kenworthy, M.K., Rittenour, T.M., Pierce, J.L., Sutfin, N.A., and Sharp, W.D., 2014, Luminescence dating without sand lenses—An application of OSL to coarse-grained alluvial fan deposits of the Lost River Range, Idaho, USA: Quaternary Geochronology, v. 23, p. 9-25.

Lahaye, C., Guibert, P., and Bechtel, F., 2012, Uranium series disequilibrium detection and annual dose determination—A case study on Magdalenian ferruginous heated sandstones (La Honteyre, France): Radiation Measurements, v. 47, no. 9, p. 786-789.

Lawson, M.J., Roder, B.J., Stang, D.M., and Rhodes, E.J., 2012, OSL and IRSL characteristics of quartz and feldspar from southern California, USA: Radiation Measurements, v. 47, no. 9, p. 830-836.

Lee, J., Spencer, J., and Owen, L., 2001, Holocene slip rates along the Owens Valley fault, California—Implications for the recent evolution of the eastern California shear zone: Geology, v. 29, no. 9, p. 819-822.

Lepper, K., Gorz, K.L., Fisher, T.G., and Lowell, T.V., 2011, Age determinations for glacial Lake Agassiz shorelines west of Fargo, North Dakota, USA: Canadian Journal of Earth Sciences, v. 48, p. 1199–1207.

Lienkaemper, J.J., and Bronk-Ramsey, C., 2009, OxCal – versatile tool for developing paleoearthquake chronologies – A primer: Seismological Research Letters, v. 80, p. 431–434.

Little, T.A., Grapes, R., and Berger, G.W., 1998, Late Quaternary strike slip on the eastern part of the Awatere fault, South Island, New Zealand: Geological Society of America Bulletin, v. 110, no. 2, p. 127-148.

Lopez, G.I., 2012, Evidence for mid-to late-Holocene palaeotsunami deposits, Kakawis Lake, Vancouver Island, British Columbia: Natural Hazards, v. 60, p. 43-68.

Lowell, T.V., 1995, The application of radiocarbon age estimates to the dating of glacial sequences—An example from the Miami sublobe, Ohio, USA: Quaternary Science Reviews, v. 14, no. 1, p. 85-99.

Mahan, S.A., Gray, H.J., Pigati, J.S., Wilson, J., Lifton, N.A., Paces, J.B., and Blaauw, M., 2014, A geochronologic framework for the Ziegler Reservoir fossil site, Snowmass Village, Colorado: Quaternary Research, v. 82, no. 3, p. 490-503, (includes extensive supplemental information), online, http://dx.doi.org/10.1016/j.yqres.2014.03.004.

Mason, D.P., Little, T.A., and Van Dissen, R.J., 2006, Rates of active faulting during late Quaternary fluvial terrace formation at Saxton River, Awatere fault, New Zealand: Geological Society of America Bulletin, v. 118, no. 11-12, p. 1431-1446.

Mayya, Y.S., Morthekai, P., Murari, M.K., and Singhvi, A.K., 2006, Towards quantifying beta microdosimetric effects in single-grain quartz dose distribution: Radiation Measurements, v. 41, no. 7, p. 1032-1039.

McAuliffe, L.J., Dolan, J.F., Kirby, E., Rollins, C., Haravitch, B., Alm, S., and Rittenour, T.M., 2013, Paleoseismology of the southern Panamint Valley fault—Implications for regional earthquake occurrence and seismic hazard in southern California: Journal of Geophysical Research—Solid Earth, v. 118, p. 5126-5146.

McCalpin, J.P., Forman, S.L., and Lowe, M., 1994, Reevaluation of Holocene faulting at the Kaysville site, Weber segment of the Wasatch fault zone, Utah: Tectonics, v. 13, no. 1, p. 1-16.

McCalpin, J., and Forman, S.L., 1991, Late Quaternary faulting and thermoluminescence dating of the East Cache fault zone, north-central Utah: Bulletin of the Seismological Society of America, v. 81, no. 1, p. 139-161.

McGill, S.F., Owen, L.A., Weldon, R.J., and Kendrick, K.J., 2013, Latest Pleistocene and Holocene slip rate for the San Bernardino strand of the San Andreas fault, Plunge Creek, Southern California—Implications for strain partitioning within the southern San Andreas fault system for the last~ 35 ky: Geological Society of America Bulletin, v. 125, no. 1-2, p. 48-72.

Menges, C.M., Taylor, E.M., Vadurro, G., Cress, R., Murray, M.H., Lundstrom, S.C., Paces, J.B., and Mahan, S.A., 1997, Logs and paleoseismic interpretations from trenches ^{14}C and ^{14}D on the Bow Ridge fault, northeastern Yucca Mountain, Nye County, Nevada: U.S. Geological Survey Miscellaneous Field Studies Map 2311 (4 plates), scale 1:25. http://pubs.er.usgs.gov/publication/mf2311.

Mukul, M., Jaiswal, M., and Singhvi, A.K., 2007, Timing of recent out-of-sequence active deformation in the frontal Himalayan wedge—Insights from the Darjiling sub-Himalaya, India: Geology, v. 35, no. 11, p. 999-1002.

Munyikwa, K., 2005, The role of dune morphogenetic history in the interpretation of linear dune luminescence chronologies—A review of linear dune dynamics: Progress in Physical Geography, v. 29, p. 317-336.

Murray, A.S., and Olley, J.M., 2002, Precision and accuracy in the optically stimulated luminescence dating of sedimentary quartz—A status review: Geochronometria, v. 21, p. 1–16.

Murray, A.S., and Roberts, R.G., 1997, Determining the burial time of single grains of quartz using optically stimulated luminescence: Earth and Planetary Science Letters, v. 152, no. 1, p. 163-180.

Murray, A.S., and Wintle, A.G., 2000, Luminescence dating of quartz using an improved single-aliquot regenerative-dose protocol: Radiation Measurements, v. 32, no. 1, p. 57-73.

Murray, A.S., and Wintle, A.G., 2003, The single aliquot regenerative dose protocol—Potential for improvements in reliability: Radiation Measurements, v. 37, no. 4, p. 377-381.

Nathan, R.P., and Mauz, B., 2008, On the dose-rate estimate of carbonate-rich sediments for trapped charge dating: Radiation Measurements, v. 43, p. 14-25.

Nelson, M.S., and Rittenour, T., 2014, Using grain-size distribution to build water retention curves for alluvial sediments—Application to dose-rate calculation, *in* 14th International Conference on Luminescence and Electron Spin Resonance Dating Book of Abstracts: Université du Québec à Montréal, Montreal, p. 146.

Olley, J.M., Murray, A., and Roberts, R.G., 1996, The effects of disequilibria in the uranium and thorium decay chains on burial dose rates in fluvial sediments: Quaternary Science Reviews, v. 15, no. 7, p. 751-760.

Olley, J.M., Caitcheon, G.G., and Roberts, R.G., 1999, The origin of dose distributions in fluvial sediments, and the prospect of dating single grains from fluvial deposits using optically stimulated luminescence: Radiation Measurements, v. 30, no. 2, p. 207-217.

Parish, R., 1994, The influence of feldspar weathering on luminescence signals and the implications for luminescence dating of sediments, *in* Robinson, D.A., and Williams, R.B.G., editors, Rock weathering and landform evolution: University of Sussex Geography Laboratory, p. 243-258.

Prescott, J.R., and Hutton, J.T., 1994, Environmental dose rates and radioactive disequilibrium from some Australian luminescence dating sites: Quaternary Science Reviews, v. 14, no. 4, p. 439-448.

Personius, S.F., and Mahan, S.A., 2000, Paleoearthquake recurrence on the East Paradise fault zone, metropolitan Albuquerque, New Mexico: Bulletin of the Seismological Society of America, v. 90, no. 2, p. 357-369.

Porat, N., Duller, G.A.T., Roberts, H.M., Piasetzky, E., and Finkelstein, I., 2012, OSL dating in multi-strata Tel—Megiddo (Israel) as a case study: Quaternary Geochronology, v. 10, p. 359-366.

Porat, N., Amit, R., Zilberman, E., and Enzel, Y., 1997, Luminescence dating of fault-related alluvial fan sediments in the southern Arava valley, Israel: Quaternary Science Reviews, v. 16, no. 3, p. 397-402.

Porat, N., Wintle, A.G., Amit, R., and Enzel, Y., 1996, Late Quaternary earthquake chronology from luminescence dating of colluvial and alluvial deposits of the Arava Valley, Israel: Quaternary Research, v. 46, no. 2, p. 107-117.

Ran, Y.K., Chen, W.S., Xu, X.W., Chen, L.C., Wang, H., Yang, C.C., and Dong, S.P., 2013, Paleoseismic events and recurrence interval along the Beichuan–Yingxiu fault of Longmenshan fault zone, Yingxiu, Sichuan, China: Tectonophysics, v. 584, no, 1 p. 81-90.

Reimann, T., Thomsen, K.J., Jain, M., Murray, A.S., and Frechen, M., 2012, Single-grain dating of young sediments using the pIRIR signal from feldspar: Quaternary Geochronology, v. 11, p. 28-41.

Rhodes, E.J., 2011, Optically stimulated luminescence dating of sediments over the past 200,000 years: Annual Review of Earth and Planetary Sciences, Annual Reviews, v. 39, p. 461-488, doi: 10.1146/annurev-earth-040610-133425.

Rittenour, T.M., 2008, Luminescence dating of fluvial deposits—Applications to geomorphic, paleoseismic, and archaeological research: Boreas, v. 37, no. 4, p. 613-635.

Rittenour, T.M., Coates, L.L., and Metcalfe, D., in press, Investigation of late and post-Fremont alluvial stratigraphy of range creek, east-central Utah—Use of OSL when radiocarbon fails: Quaternary International.

Rockwell, T.K., Lindvall, S., Herzberg, M., Murbach, D., Dawson, T., and Berger, G., 2000, Paleoseismology of the Johnson Valley, Kickapoo, and Homestead Valley faults— Clustering of earthquakes in the eastern California shear zone: Bulletin of the Seismological Society of America, v. 90, no. 5, p. 1200-1236.

Sawakuchi, A.O., Blair, M.W., DeWitt, R., Faleiros, F.M., Hyppolito, T., and Guedes, C.C.F., 2011, Thermal history versus sedimentary history—OSL sensitivity of quartz grains extracted from rocks and sediments: Quaternary Geochronology, v. 6, p. 261-272.

Sohn, M.F., Knott, J.R., and Mahan, S.A., 2014, Paleoseismology of the southern section of the Black Mountains and Southern Death Valley fault zones, Death Valley, United States: Environmental and Engineering Geoscience, v. 20, no. 2, p. 177-198.

Stafford, T.W., and Forman, S.L., 1993, Radiocarbon and thermoluminescence dating of Wasatch faulting events, Gardner Canyon, Utah: Utah Geological Survey Contract Report 93-4, 15 p.

Trumbore, S.E., 2000, Radiocarbon geochronology, *in* Sowers, J.M., Noller, J.S., and Lettis, W.R., editors, Quaternary geochronology, methods and applications: American Geophysical Union, Reference Shelf 4, p. 157–176.

Vermeesch, P., 2009, RadialPlotter—A Java application for fission track, luminescence, and other radial plots: Radiation Measurements, v. 44, no. 4, p. 409-410.

Wallinga, J., Murray, A., and Wintle, A., 2000, The single-aliquot regenerative-dose (SAR) protocol applied to coarse-grain feldspar: Radiation Measurements, v. 32, no. 5, p. 529-533.

Wallinga, J., 2002, Optically stimulated luminescence dating of fluvial deposits—A review: Boreas, v. 31, no. 4, p. 303-322.

Wang, X.L., Wintle, A.G., and Lu, Y.C., 2006, Thermally transferred luminescence in fine-grained quartz from Chinese loess—Basic observations: Radiation Measurements, v. 41, no. 6, p. 649-658.

Wintle, A.G., and Huntley, D.J., 1982, Thermoluminescence dating of sediments: Quaternary Science Reviews, v. 1, no. 1, p. 31-53.

Wintle, A.G., and Murray, A.S., 2006, A review of quartz optically stimulated luminescence characteristics and their relevance in single-aliquot regeneration dating protocols: Radiation Measurements, v. 41, no. 4, p. 369-391.

Zilberman, E., Amit, R., Heimann, A., and Porat, N., 2000, Changes in Holocene paleoseismic activity in the Hula pull-apart basin, Dead Sea Rift, northern Israel: Tectonophysics, v. 321, no. 2, p. 237-252.

Zreda, M.G., and Phillips, F.M., 2000, Cosmogenic nuclide buildup in surficial materials, *in* Sowers, J.M., Noller, J.S., and Lettis, W.R., editors, Quaternary geochronology, methods and applications: American Geophysical Union, Reference Shelf 4, p. 61–76.

Zuchiewicz, W., Cuong, N.Q., Bluszcz, A., and Michalik, M., 2004, Quaternary sediments in the Dien Bien Phu fault zone, NW Vietnam—A record of young tectonic processes in the light of OSL-SAR dating results: Geomorphology, v. 60, no. 3, p. 269-302.